Magnetic field control of plasmon polaritons in graphene-covered gyrotropic planar waveguide

Dmitry A. Kuzmin,[1,*] Igor V. Bychkov,[1] and Vladimir G. Shavrov[2]

[1]*Chelyabinsk State University, 129 Br. Kashirinykh St., Chelyabinsk 454001, Russian Federation*

[2]*Kotelnikov Institute of Radio-Engineering and Electronics of RAS, 11/7 Mokhovaya St., Moscow 125009, Russian Federation*

**Corresponding author: kuzminda89@gmail.com*

Received April 20, 2015; revised May 5, 2015; accepted May 5, 2015;
posted May 8, 2015 (Doc. ID 238388); published May 22, 2015

In this Letter, we report about magnetic field switching of plasmon polaritons propagating into a planar gyrotropic waveguide covered by two graphene layers at a deeply subwavelength scale. It is shown that applying an external magnetic field may lead to energy redistribution between two waveguide surfaces. The effect value resonantly depends on the relation between waveguide size and exciting light wavelength. A change in chemical potential of graphene layers may be used for tuning the phase shift between plasmon polaritons at near-resonant wavelengths. Evident effect may be observed at low magnetic fields (less than one tesla) for wavelengths about microns on a scale of tens of nanometers. Such an effect may be used for plasmonics, photonics. and optoelectronics devices, as well as sensing applications.

OCIS codes: (240.6680) Surface plasmons; (250.5403) Plasmonics; (250.6715) Switching; (230.3810) Magneto-optic systems.

http://dx.doi.org/10.1364/OL.40.002557

Today graphene attracts great researchers' attention in plasmonics. In contradiction to metal-based plasmonics, it may support both TE- and TM- surface plasmon polaritons (SPPs) [1–9]. Multilayer graphene-based structures may be used like hyperbolic metamaterials [10,11]; they may support deeply subwavelength surface modes [12]; heterointerface of graphene sheet arrays may have negative plasmon refraction [13]. Most authors consider only simple dielectric medium, where graphene layer (GL) is placed. We know of only a few theoretical works in which authors investigated GLs with more complex substrates [14–16]. Recently, GL on yttrium iron garnet film has been fabricated [17]. While the magnetic properties of GL were interesting, such a structure may open wide perspectives for graphene-based magnetoplasmonics devices. Magneto-optical properties of GLs in a magnetic field directed perpendicularly to its surface are well known [18–20], but they are nonsensitive to an in-plane magnetic field. Recently, we have demonstrated that graphene may affect magnetic speckle-pattern rotation of light in gyrotropic optical fiber significantly, even in the case of quartz fiber with low gyrotropy [21]. An investigation of substrate gyrotropy influence on plasmonic properties of GL may be quite interesting.

It is well known from microwave techniques, that in rectangular waveguides filled by transversely magnetized ferrites, electromagnetic energy has a lack of reflection symmetry along an axis perpendicular to both external magnetic field and guiding wave direction [22–24]. One may hope that a similar effect will take place in planar gyrotropic waveguide at infrared or optical frequencies. In the case of an SPPs waveguide, we may expect plasmon energy redistribution between two guiding surfaces. Such an effect may be used for plasmonics, photonics, and optoelectronics device, as well as sensing applications. Waveguide properties of double GLs have been investigated earlier [25–29]. In this work we investigate magnetic field control of infrared and optical SPPs in double GL-based plasmonic waveguides filled by magnetized gyrotropic medium.

Let us consider plasmonic waveguide formed by two GLs filled by gyrotropic core at $0 < x < a$, where a is a distance between GLs. Let us assume that top and bottom mediums (shell of the waveguide) are equals and have gyrotropy too. Such a waveguide is placed in an external magnetic field $\mathbf{H}$ lying in the plane of GLs. Coordinate axes are chosen in such a way that the y-axis coincides with the SPPs propagation direction; z-axis coincides with the magnetic field direction (i.e., $\mathbf{H} = (0, 0, H_0)$). The scheme is shown in Fig. 1.

Let the electromagnetic field with harmonic time-dependence ($\sim \exp(i\omega t)$) propagate in the system along the y-axis ($\sim \exp(-i\beta y)$, where β is the propagation constant). Electrodynamic properties of the gyrotropic core and shell may be described by electric permittivity tensors:

$$\hat{\varepsilon}_{c,sh} = \begin{pmatrix} \varepsilon_{c,sh} & i\varepsilon_{a\ c,sh} & 0 \\ -i\varepsilon_{a\ c,sh} & \varepsilon_{c,sh} & 0 \\ 0 & 0 & \varepsilon_{||c,sh} \end{pmatrix}. \quad (1)$$

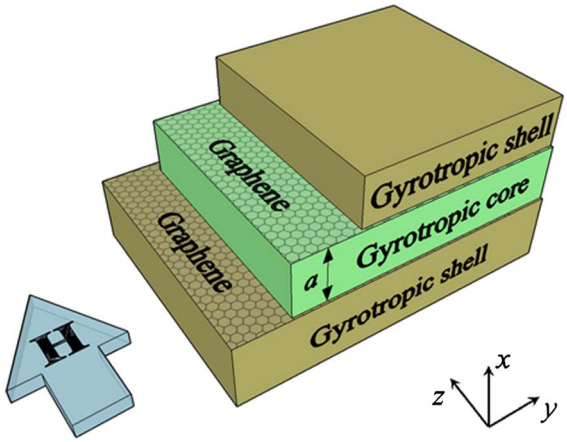

Fig. 1. Scheme of bilayer graphene waveguide with a gyrotropic core and shell.

GLs may be represented as infinitely thick conductive surfaces [4]. Conductivity of GL σ has been considered in many works [4,19,30–32]. We will use the expression resulting from the Kubo formula [33]. In the present work, it is essential that σ depends on chemical potential which, for example, may be changed easily by gate voltage. In chosen geometry, gyrotropy affects only TM-modes of the waveguide. Using Maxwell's equations, one may derive tangential components of electromagnetic fields in the form $H_z(x,y) = H_{z\beta}(x)\exp[-i\beta y]$, $E_y(x,y) = E_{y\beta}(x)\exp[-i\beta y]$, where

$$H_{z\beta}(x) = \begin{cases} A\exp(-\gamma x), x \geq a \\ B\exp(\zeta x) + C\exp(-\zeta x), 0 < x < a \\ D\exp(\gamma x), x \leq 0 \end{cases}$$

$$E_{y\beta}(x) = \begin{cases} i\gamma_+ A\exp(-\gamma x)/k_0\varepsilon_{\perp sh}, x \geq a \\ i[\zeta_+ C\exp(-\zeta x) - \zeta_- B\exp(\zeta x)]/k_0\varepsilon_{\perp c}, 0 < x < a \\ -i\gamma_- D\exp(\gamma x)/k_0\varepsilon_{\perp sh}, x \leq 0. \end{cases} \quad (2)$$

In Eq. (2) the following notation has been introduced: $\gamma_\pm = \gamma \pm \beta\varepsilon_{a\,sh}/\varepsilon_{sh}$, $\zeta_\pm = \zeta \pm \beta\varepsilon_{a\,c}/\varepsilon_c$, $k_0 = \omega/c = 2\pi/\lambda$, $\varepsilon_{\perp sh,c} = \varepsilon_{sh,c} - \varepsilon^2_{a\,sh,c}/\varepsilon_{sh,c}$. c is the speed of light in vacuum; λ is the wavelength of exciting light; γ, $\zeta = (\beta^2 - k_0^2\varepsilon_{\perp sh,c})^{1/2}$ are the constants of SPPs localization. Fields (2) should satisfy the boundary conditions

$$(\mathbf{E_1} - \mathbf{E_2}) \times \mathbf{n_{12}} = 0, (\mathbf{H_1} - \mathbf{H_2}) \times \mathbf{n_{12}} = 4\pi\mathbf{j_g}/c, \quad (3)$$

where $\mathbf{n_{12}}$ is normal vector directed from medium "1" to medium "2" and $\mathbf{j_g}$ is the surface current density in GLs. Putting fields (2) into conditions (3), we will derive a system of equations for field amplitudes A, B, C, and D. From this system one may get the dispersion equation for surface plasmon polaritons:

$$\exp(\zeta a)(\varepsilon_{\perp c}\gamma_+ + \varepsilon_{\perp sh}\zeta_-\Phi_+)(\varepsilon_{\perp c}\gamma_- + \varepsilon_{\perp sh}\zeta_+\Phi_-) = \exp(-\zeta a)(\varepsilon_{\perp c}\gamma_+ - \varepsilon_{\perp sh}\zeta_+\Phi_+)(\varepsilon_{\perp c}\gamma_- - \varepsilon_{\perp sh}\zeta_-\Phi_-),$$
$$\Phi_\pm = 1 - 4i\pi\sigma\gamma_\pm/ck_0\varepsilon_{\perp sh}. \quad (4)$$

Equation (4) yields a propagation constant β. With β we may calculate localization constants γ, ζ, and determine the field distribution from (2). This equation is difficult for analysis, and may be solved only by numerical methods.

To characterize SPPs redistribution we will introduce the following parameter:

$$\eta = \frac{E_{y\beta}(a)}{E_{y\beta}(0)} = \frac{-\Phi_-\gamma_+\zeta\varepsilon_{\perp sh}\gamma_-^{-1}}{(\varepsilon_{\perp c}\gamma_+ - \Phi_+\beta\varepsilon_{\perp sh}\varepsilon_{a\,c}/\varepsilon_c)\mathrm{sh}(\zeta a) + \zeta\varepsilon_{\perp sh}\Phi_+\mathrm{ch}(\zeta a)}. \quad (5)$$

In general, η has complex values and may be expressed as $\eta = |\eta|\exp(i\varphi)$, where $|\eta|$ means rate between amplitudes and φ is a phase shift for SPPs on the top and bottom graphene layers.

It is easy to show that, for a nongyrotropic core and shell, there may be two TM-modes (symmetric and asymmetric), and $\eta = \pm 1$. The dispersion equation cannot be split into symmetric and asymmetric modes if only waveguide core is gyrotropic. Equation (5), if taking into account dispersion Eq. (4), may be transformed:

$$\eta = \pm\sqrt{\frac{(\varepsilon_{\perp c}\gamma + \Phi\beta\varepsilon_{sh}\varepsilon_{a\,c}/\varepsilon_c)^2 - (\zeta\varepsilon_{sh}\Phi)^2}{(\varepsilon_{\perp c}\gamma - \Phi\beta\varepsilon_{sh}\varepsilon_{a\,c}/\varepsilon_c)^2 - (\zeta\varepsilon_{sh}\Phi)^2}}. \quad (6)$$

From Eq. (6), we may conclude that there are only few nontrivial cases in which the effect of energy redistribution is absent. The first one, when $\varepsilon_{a\,c} = 0$, we have just discussed. The second one corresponds to the condition $\Phi = 1 - 4i\pi\sigma\gamma/ck_0\varepsilon_{sh} = 0$. Energy redistribution will take place, even for $\Phi = 0$, if we assume that both core and shell are gyrotropic.

For numerical calculations, let us assume for graphene conductivity that scattering rate $\Gamma \sim 1$ meV at temperature $T = 300$ K [34]. In recent experiments, the chemical potential of GLs μ_{ch} has reached as high as 1.17 eV [35]. For definiteness, we will assume that μ_{ch} variation is of n-type. We will consider only the symmetric waveguide, when top and bottom GLs have the same conductivity σ (μ_{ch} are equals). An anti-symmetric waveguide will have some features, and should be investigated separately. For the core and shell of the waveguide, we will use the parameters of Bi-doped YIG. It has great gyrotropy, and is frequently used for magneto-optical applications. In addition, a small change in Bi-doping level should lead to a small change in refractive index and gyrotropy of material. Verde constants of core and shell will be considered as equals. They define an antisymmetric part of the electric permittivity $\varepsilon_a = VH_0\lambda\varepsilon^{1/2}/\pi$. Bi-doped YIG has $V \sim 10^{-6}$ rad/(Gs μm) [36]. A wavelength of light in a vacuum will be set as $\lambda = 1.5$ μm (the wavelength of erbium-doped fiber lasers radiation frequently used for fiber-optic communication). The refractive indexes of core and shell will put $n_c = (\varepsilon_c)^{1/2} = 2.36$ and $n_{sh} = (\varepsilon_{sh})^{1/2} = 2.34$.

An analysis showed that, for such parameter values, only the quasi-antisymmetric mode may exist for waveguide sizes not more than ~10 nm. Typical electric field distributions for $a = 100$ nm, $\mu_{ch} = 1$ eV, and magnetic field values $H = 0, \pm 1$ T are shown on Fig. 2. One can see that guided waves are weakly localized (localization constant $\mathrm{Re}[\gamma] \approx 0.08$ μm^{-1}). The ratio between amplitudes reaches about 2.

Calculations show that localization of guiding waves depends on the waveguide size and difference between core and shell refractive indexes. Thus, for the same difference of refractive indexes, but for a five times wider waveguide ($a = 500$ nm), the localization parameter is greater: $\mathrm{Re}[\gamma] \approx 0.38$ μm^{-1}. For this size, ratio between amplitudes reaches only 1.2. On the other hand, for a waveguide with $a = 100$ nm, but $n_{sh} = 2.30$, we will have $\mathrm{Re}[\gamma] \approx 0.23$ μm^{-1} and the redistribution effect value is only about 1.3.

Let us examine in detail how the effect depends on waveguide size and magnetic field value. Figure 3 shows results of the calculations. One can see that a decrease in waveguide size leads to an increase in $|\eta|$. Thus, for a

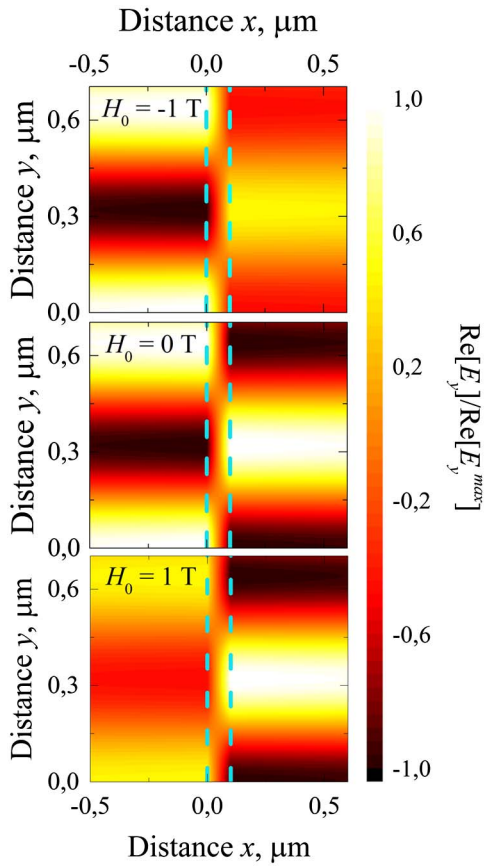

Fig. 2. Typical electric field distributions. Dashed lines show the graphene layer position. The waveguide size $a =$ 100 nm; the graphene chemical potential $\mu_{ch} = 1$ eV; and the wavelength of the exciting wave $\lambda = 1.5$ μm.

waveguide size of ~10 nm, $|\eta|$ may reach 2, even in sufficiently low magnetic fields of 1 kOe. As we have pointed out earlier, SPPs are localized weakly for a smaller waveguide. An increase in magnetic field leads to an increase of $|\eta|$, and has no effect on SPPs localization. We should note also that there is some critical relation between wavelength and waveguide size, when the quasi-antisymmetric mode becomes quasi-symmetric. This corresponds to the phase shift φ change from $\pm\pi$ to zero. A calculation shows that, for such a critical relation, $|\eta|$ reaches a maximum, i.e., SPPs are localized near only one of the waveguide surfaces.

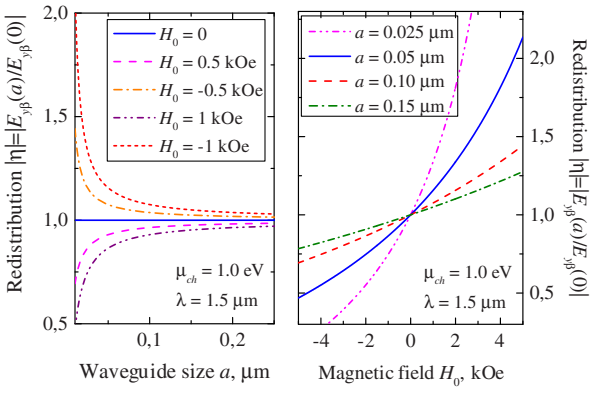

Fig. 3. Dependence of redistribution effect on the waveguide size a and the magnetic field value H_0.

Let us now investigate the influence of GLs chemical potential variation and exciting light wavelength on the redistribution effect. Indeed, refractive indexes and Verdet constants of core and shell will depend on exciting light wavelength. For simplicity of calculations and interpretation of the results, we will neglect core and shell dispersion properties. We will consider a wavelength range of 500 nm $< \lambda <$ 2.0 μm. It covers some part of visible light and near-infrared radiation. Results of the calculations are shown in Fig. 4. One can see some features we have mentioned above. At some wavelength, which is critical for chosen size of the waveguide, the quasi-antisymmetric mode (with φ near $\pm\pi$) becomes quasi-symmetric one (with φ near 0). At the same wavelength, $|\eta|$ reaches a maximum: in a magnetic field directed along the z-axis, SPPs propagating along the y-axis are localized at $x = a$, while in a magnetic field of the opposite direction they will be localized at $x = 0$. Variation of the GLs' chemical potential leads to the shift of this critical wavelength. Despite the small effect of chemical potential variation on $|\eta|$ at wavelengths far from the critical one, at a critical wavelength it may change $|\eta|$ in some magnitude orders. In addition, decreasing the GLs' chemical potential changes the wavelength's range of transition from a quasi-antisymmetric SPPs mode to a wider quasi-symmetric one. This gives us possibility to control both redistribution and the

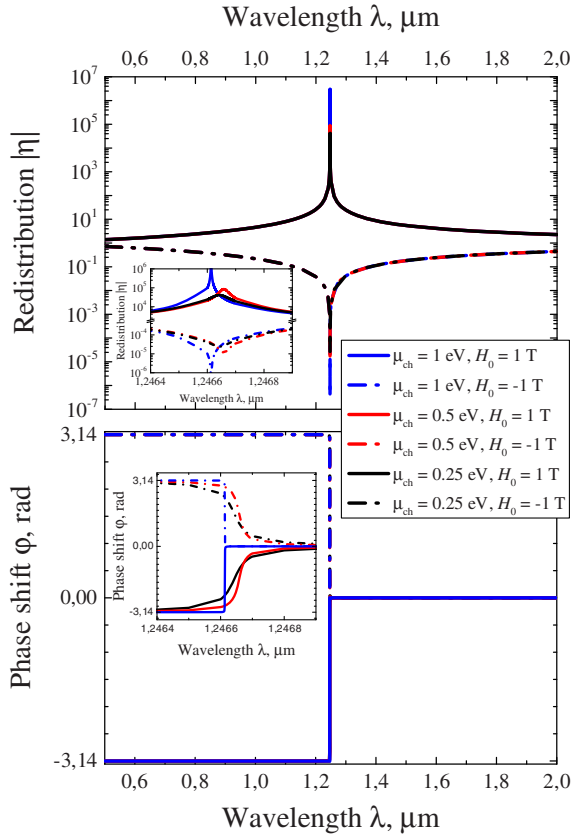

Fig. 4. Dependence of redistribution effect on the exciting light wavelength for different values of chemical potential. The insets show the wavelength range near the critical behavior. The waveguide size $a = 25$ nm.

SPPs phase by chemical potential of GLs at wavelengths near the critical one. We wish to emphasize the fact that almost full redistribution ($|\eta| \sim 10^{\pm 6}$) may be reached for a wavelength $\lambda \approx 1.246$–1.247 μm in a highly subwavelength scale of only 25 nm.

An imaginary part of the GLs' conductivity changes the sign when the frequency ω lies in the window $1.667 < \hbar\omega/\mu_{ch} < 2$ because of interband absorption. At such frequencies (or chemical potentials), a single GL cannot support a TM-mode of SPPs. In our calculations, this situation corresponds to $\mu_{ch} = 0.5$ eV, while at $\mu_{ch} = 0.25$ eV and at $\mu_{ch} = 1.00$ eV we have $\hbar\omega/\mu_{ch} > 2$ and $\hbar\omega/\mu_{ch} < 1.667$, consequently. At high frequencies (low μ_{ch}), GLs are almost transparent, the structure resulting from small size cannot support well a localized guiding mode (it becomes an optical planar waveguide working in a sub-critical regime), and one can see small broad peaks in Fig. 4. At low frequencies, only Drude-like intraband conductivity is significant. At such frequencies, the GL behaves like a metal nanocoating, but with some order of magnitude lower conductivity; SPPs are better localized in the structure, and we can see a sharp peak in Fig. 4. Effective refractive index is varied by GLs, when $1.667 < \hbar\omega/\mu_{ch} < 2$. This change leads to a small shift of the critical wavelength. A negligibly small shift of the critical wavelength due to variation of μ_{ch} may be explained by small GL conductivity at the frequencies under consideration. GL has a higher conductivity at THz and microwave frequencies, but at such frequencies gyrotropy of dielectric permittivity of substrate becomes negligible.

It is notable that a change of SPPs propagation in the opposite direction without changing the magnetic field will also lead to SPPs relocalization. Magnetic field and SPPs propagation directions are coupled by $\zeta_{\pm}$ and $\gamma_{\pm}$ in Eq. (2), which contain the term with $\beta\varepsilon_a$. Thus, if only propagation or magnetic field direction will be reversed (only sign of ε_a or β), SPPs will change the localization surface. In the case of both directions changed, we will not observe any redistribution effect.

Finally, we have proposed and theoretically investigated the possibility of magnetic field control of SPPs in a GL-covered gyrotropic planar waveguide. Investigation showed that SPPs may be switched from one GL to another by low magnetic fields. The effect resonantly depends on the relation between the waveguide size and the exciting electromagnetic wave wavelength. Change in chemical potential of GLs leads to a small shift in resonant wavelength, and tunes the effect value and SPPs phase shift. Investigated effect should sustain even if we change GL to another two-dimensional (or quasi-two-dimensional) conductive layer. A shift of the critical wavelength may be greater if it is material with higher conductivity. However, as we know, GL may support SPPs with the greatest propagation length. Investigated features make the proposed structure promising for both nanoscale light control and sensing applications.

The model development has been supported by a grant of the Russian Science Foundation no. 14-22-00279. Numerical calculation was partially supported by a grant of the Russian Foundation for Basic Research no. 13-07-00462.

References

1. R. R. Nair, P. Blake, A. N. Grigorenko, K. S. Novoselov, T. J. Booth, T. Stauber, N. M. R. Peres, and A. K. Geim, Science **320**, 1308 (2008).
2. F. Bonaccorso, Z. Sun, T. Hasan, and A. C. Ferrari, Nat. Photonics **4**, 611 (2010).
3. Q. Bao and K. P. Loh, ACS Nano **6**, 3677 (2012).
4. S. A. Mikhailov and K. Ziegler, Phys. Rev. Lett. **99**, 016803 (2007).
5. Y. V. Bludov, M. I. Vasilevskiy, and N. M. R. Peres, Eur. Phys. Lett. **92**, 68001 (2010).
6. F. H. L. Koppens, D. E. Chang, and F. J. G. de Abajo, Nano Lett. **11**, 3370 (2011).
7. A. Vakil and N. Engheta, Science **332**, 1291 (2011).
8. B. E. Sernelius, Phys. Rev. B **85**, 195427 (2012).
9. F. J. G. de Abajo, ACS Photon. **1**, 135 (2014).
10. I. V. Iorsh, I. S. Mukhin, I. V. Shadrivov, P. A. Belov, and Y. S. Kivshar, Phys. Rev. B **87**, 075416 (2013).
11. M. A. K. Othman, C. Guclu, and F. Capolino, Opt. Express **21**, 7614 (2013).
12. D. Smirnova, P. Buslaev, I. Iorsh, I. V. Shadrivov, P. A. Belov, and Y. S. Kivshar, Phys. Rev. B **89**, 245414 (2014).
13. H. Huang, B. Wang, H. Long, K. Wang, and P. Lu, Opt. Lett. **39**, 5957 (2014).
14. A. Madani, S. Zhong, H. Tajalli, S. R. Entezar, A. Namdar, and Y. Ma, Prog. Electromagn. Res. **143**, 545 (2013).
15. D. A. Kuzmin, I. V. Bychkov, and V. G. Shavrov, Photonics Nanostruct. Fundam. Appl. **12**, 473 (2014).
16. D. A. Kuzmin, I. V. Bychkov, and V. G. Shavrov, IEEE Trans. Magn. **50**, 1 (2014).
17. Z. Wang, C. Tang, R. Sachs, Y. Barlas, and J. Shi, Phys. Rev. Lett. **114**, 016603 (2015).
18. M. Orlita, C. Faugeras, J. Borysiuk, J. M. Baranowski, W. Strupiński, M. Sprinkle, C. Berger, W. A. de Heer, D. M. Basko, G. Martinez, and M. Potemski, Phys. Rev. B **83**, 125302 (2011).
19. L. A. Falkovsky, Phys. Usp. **55**, 1140 (2012).
20. I. Crassee, M. Orlita, M. Potemski, A. L. Walter, M. Ostler, T. Seyller, I. Gaponenko, J. Chen, and A. B. Kuzmenko, Nano Lett. **12**, 2470 (2012).
21. D. A. Kuzmin, I. V. Bychkov, and V. G. Shavrov, Opt. Lett. **40**, 890 (2015).
22. A. L. Mikaelyan, Dokl. Akad. Nauk. USSR **98**, 941 (1954).
23. G. Barzilai and G. Gerosa, Il Nuovo Cimento **7**, 685 (1958).
24. A. G. Gurevich and G. A. Melkov, *Magnetization Oscillations and Waves* (CRC Press, 1996).
25. G. W. Hanson, J. Appl. Phys. **103**, 064302 (2008).
26. C. H. Gan, H. S. Chu, and E. P. Li, Phys. Rev. B **85**, 125431 (2012).
27. M. Liu, X. Yin, and X. Zhang, Nano Lett. **12**, 1482 (2012).
28. P. I. Buslaev, I. V. Iorsh, I. V. Shadrivov, P. A. Belov, and Y. S. Kivshar, J. Eng. Theor Phys. Lett. **97**, 535 (2013).
29. D. Svintsov, V. Vyurkov, V. Ryzhii, and T. Otsuji, J. Appl. Phys. **113**, 053701 (2013).
30. L. A. Falkovsky and S. S. Pershoguba, Phys. Rev. B **76**, 153410 (2007).
31. V. P. Gusynin and S. G. Sharapov, Phys. Rev. B **73**, 245411 (2006).
32. L. A. Falkovsky and A. A. Varlamov, Eur. Phys. J. B **56**, 281 (2007).
33. V. P. Gusynin, S. G. Sharapov, and J. P. Carbotte, J. Phys. **19**, 026222 (2007).
34. J. Y. Kim, C. Lee, S. Bae, K. S. Kim, B. H. Hong, and E. J. Choi, Appl. Phys. Lett. **98**, 201907 (2011).
35. D. K. Efetov and P. Kim, Phys. Rev. Lett. **105**, 256805 (2010).
36. A. K. Zvezdin and V. A. Kotov, *Modern Magneto-Optics and Magneto-Optical Materials* (IOP, 1997).